Competition between cubic and uniaxial anisotropy in $Ga_{1-x}Mn_xAs$ in the low-Mn-concentration limit

L. V. Titova,[1] M. Kutrowski,[1,2] X. Liu,[1] R. Chakarvorty,[1] W. L. Lim,[1] T. Wojtowicz,[1,2] J. K. Furdyna,[1] and M. Dobrowolska[1,*]
[1]*Department of Physics, University of Notre Dame, Notre Dame, Indiana 46556, USA*
[2]*Institute of Physics, Polish Academy of Sciences, 02-668 Warsaw, Poland*
(Received 1 July 2005; published 28 October 2005)

We have studied the dependence of the cubic and uniaxial magnetic anisotropy terms in $Ga_{1-x}Mn_xAs$ on temperature T and hole concentration p. For the purpose of this study we prepared a series of $Ga_{1-x}Mn_xAs$ layers with low Mn concentration ($x \approx 0.01$), codoped by Be in the range $3.0\times10^{19} < p < 8.5\times10^{19}$ cm^{-3}, and grown on hybrid ZnSe/GaAs substrates. The use of such hybrid substrates was intended to obtain $Ga_{1-x}Mn_xAs$ layers in which—due to the small lattice mismatch between $Ga_{0.99}Mn_{0.01}As$ and ZnSe—the uniaxial and the cubic anisotropy terms are comparable, so that the contributions of both types of anisotropy could be investigated. The effects of magnetic anisotropy were studied by polar magneto-optical Kerr effect, which allowed us to monitor the reversal process of perpendicular magnetization. The results showed that cubic anisotropy is highly sensitive to both p and T. Specifically, we have found that in samples with high p the cubic anisotropy term is dominant at low T, but decreases rapidly as T increases. In sharp contrast, uniaxial anisotropy shows only a weak dependence on p and T, thus dominating at temperatures close to T_C even in samples with high p. These results show that magnetic anisotropy and the magnetization reversal process in $Ga_{1-x}Mn_xAs$ can be engineered by an appropriate choice of the temperature and carrier concentration.

DOI: 10.1103/PhysRevB.72.165205 PACS number(s): 75.50.Pp, 78.20.Ls, 78.66.Fd, 75.60.Jk

I. INTRODUCTION

In order to take advantage of the magnetic properties of $III_{1-x}Mn_xV$ ferromagnetic (FM) semiconductor alloys in spin-based devices, the process of magnetization reversal has to be well understood. Unlike ferromagnetic metals, in ferromagnetic semiconductors such as $Ga_{1-x}Mn_xAs$ the demagnetization field is quite small due to the fact that the magnetic ions in these systems are quite diluted.[1,2] Consequently, magnetocrystalline anisotropy plays a decisive role in the process of magnetization reversal. This is true for both configurations that are generally of interest: in-plane, when the magnetic field is applied parallel to the ferromagnetic layer; and perpendicular, when the field is applied normal to the layer plane. In order to be able to design spin-based devices using ferromagnetic $III_{1-x}Mn_xV$ semiconductor alloys, it is therefore essential to understand the behavior of magnetic anisotropy in this family of materials. In addition, it has been observed that magnetic properties of $III_{1-x}Mn_xV$ alloys can be externally manipulated by doping, by applying an electric field, or by varying the temperature.[3–6] These findings make $III_{1-x}Mn_xV$ ferromagnetic semiconductors attractive as potential candidates for magnetic logic devices.

In the context of our current understanding of magnetic anisotropy in thin $III_{1-x}Mn_xV$ layers, the in-plane anisotropy and the in-plane magnetization reversal have already been studied rather thoroughly by several research groups.[7–10] In this configuration different hysteresis loops have been observed by standard magnetization measurements[9] and/or by longitudinal magneto-optical Kerr effect (MOKE)[8] when the external magnetic field H is applied along the three high-symmetry in-plane crystal axes: [110], [1$\bar{1}$0] and [100] (here the [001] direction is taken as the normal to the layer plane). Moreover, precise values of the cubic and uniaxial magnetic anisotropy fields were determined by ferromagnetic resonance experiments.[7] Finally, magneto-optical imaging was also used to visually reveal the in-plane magnetization reversal process in $Ga_{1-x}Mn_xAs$ films, i.e., the nucleation and propagation of domains when H is applied in the plane of the sample.[11]

In contrast, experimental studies of the out-of-plane magnetization and its anisotropy parameters are far from complete, and this will be the main focus of the present paper. Our intention is to investigate this in $Ga_{1-x}Mn_xAs$, since this material is the most thoroughly understood; but the results obtained are expected to apply in principle to $III_{1-x}Mn_xV$ ferromagnetic semiconductors generally. In this study we choose $Ga_{1-x}Mn_xAs$ with a low Mn concentration ($x \approx 0.01$) grown on ZnSe buffer layers. $Ga_{1-x}Mn_xAs$ with a low value of x is interesting for several reasons. First, it gives us the opportunity to study magnetic anisotropy at the very onset of ferromagnetism in $III_{1-x}Mn_xV$ alloys. Second, at $x \approx 0.01$ the biaxial strain in the $Ga_{1-x}Mn_xAs$ layer is small, since the lattice constant of ZnSe exceeds that of $Ga_{0.99}Mn_{0.01}As$ by only a very small amount. As a result, the strain-induced uniaxial anisotropy in these specimens is relatively small. Therefore—unlike $Ga_{1-x}Mn_xAs$ specimens studied in most investigations ($x \geqslant 0.05$ grown directly on GaAs substrates, where the perpendicular magnetization reversal is overwhelmingly dominated by uniaxial anisotropy)—thin $Ga_{1-x}Mn_xAs$ films with $x \approx 0.01$ grown on hybrid ZnSe/GaAs substrates are unique in that the uniaxial and the cubic anisotropy terms are comparable in magnitude, thus enabling us to study the competition between these anisotropy components. In particular, since the cubic and uniaxial anisotropies are observed to have different dependences on temperature T and on the hole concentration p, one can change their relationship by varying T and/or p, and

by these means manipulate the magnetization reversal in a controlled fashion.

II. EXPERIMENT AND SAMPLE CHARACTERISTICS

We have strategically designed $Ga_{1-x}Mn_xAs$ samples where magnetic anisotropy parameters can be varied by doping and/or by the temperature. A series of 300 nm thick $Ga_{1-x}Mn_xAs$ layers ($x \approx 0.01$) were grown by molecular beam epitaxy (MBE) on 300 nm ZnSe buffers which were previously deposited on GaAs substrates. During the growth of $Ga_{1-x}Mn_xAs$ the substrate temperature was kept at $T_S = 270$ °C. X-ray diffraction measurements show that the ZnSe buffers used in the growth were not fully relaxed. As a result the biaxial strain in the $Ga_{1-x}Mn_xAs$ layers, while still tensile, is very small ($\varepsilon_{xx} \leqslant 0.001$, about half of the strain of $Ga_{0.99}Mn_{0.01}As$ grown on a fully-relaxed ZnSe buffer with thickness of 4 μm).[12] During the $Ga_{1-x}Mn_xAs$ deposition the temperature of the Mn effusion cell in the MBE growth chamber was kept constant ($T_{Mn} = 700$ °C), yielding approximately a 1% Mn concentration ($x \approx 0.01$) in the $Ga_{1-x}Mn_xAs$ layers.

In order to vary the hole concentration, the $Ga_{1-x}Mn_xAs$ layers were codoped with Be during the growth, the resulting apparent hole concentration ranging from $p = 3.0 \times 10^{19}$ cm^{-3} to 8.5×10^{19} cm^{-3}, as determined by room temperature Hall measurements.[13] Although the carrier densities obtained from Hall measurements are not rigorously valid due to the contribution of the anomalous Hall effect, they nevertheless provide a useful indication of the *relative* hole concentration level, particularly in the limit of low x.[14]

As an experimental method for studying the perpendicular component of the magnetization (and thus the perpendicular magnetic anisotropy terms) we have chosen the polar magneto-optical Kerr effect (PMOKE), since this method offers important advantages. First, the Kerr rotation angle measured at normal incidence is a linear function of the normal component of the magnetization of the sample,[15] thus making it ideally suited for studying the behavior of the out-of-plane magnetization. Second, the Kerr signal, although quite small, can be recovered from the noise by means of piezoelectric modulation of polarization and the lock-in detection. And third, unlike the case of direct magnetization measurement (e.g., SQUID), PMOKE is not overshadowed by the diamagnetic signal from the GaAs substrate in the studied samples. The latter two advantages are especially important for samples with small Mn concentrations, such as those investigated in this paper. The experimental PMOKE apparatus used in the present investigation is identical to that described in the recent article by Lang *et al.*[16]

In what follows, we will use PMOKE as a measure of the projection of the magnetization on the normal to the $Ga_{1-x}Mn_xAs$ layer, which will allow us to deduce information on the anisotropy parameters that dominate the behavior of perpendicular magnetization and its reversal in $Ga_{1-x}Mn_xAs$. In the process we will also attempt to establish how these parameters can be engineered and controlled.

III. EXPERIMENTAL RESULTS

Figure 1 shows PMOKE data taken at 7 K plotted as a function of the applied magnetic field H for a series of four $Ga_{1-x}Mn_xAs$ samples with different hole concentrations: $p = 3.0 \times 10^{19}$, 3.4×10^{19}, 4.4×10^{19}, and 8.5×10^{19} cm^{-3}. The corresponding Curie temperatures of these four samples are 12 K, 16 K, 20 K, and 26 K, respectively. Note that in the high field limit all PMOKE data show a small but finite slope that varies linearly with H, which may be attributed to the paramagnetic contribution from isolated Mn spins to the total magnetization. At low fields, however, all M vs H curves initially increase sharply as the field increases, saturating at $H \approx 0.5$ kOe for all four specimens. We attribute the behavior of magnetization shown in Fig. 1 to the specific properties of magnetic anisotropy of the four $Ga_{1-x}Mn_xAs$ films.

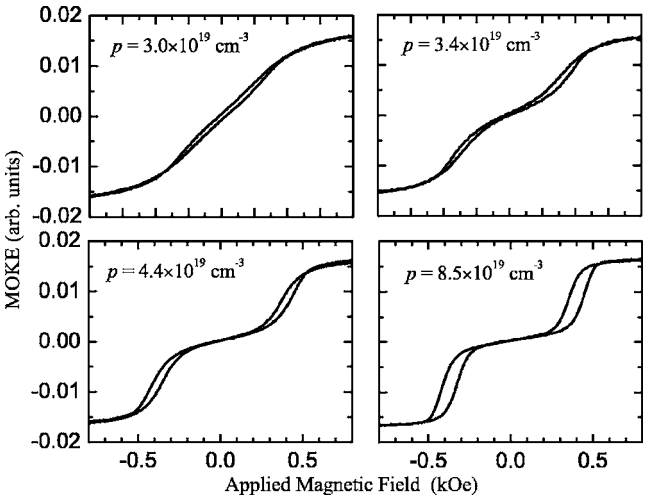

FIG. 1. Magnetic field dependence of the PMOKE signal at 7.0 K for samples with various hole concentrations.

It is generally accepted that the magnetic anisotropy of $Ga_{1-x}Mn_xAs$ films is largely controlled by epitaxial strain, tensile and compressive strains inducing in-plane and out-of-plane magnetic moment orientations, respectively.[17–19] Although all four $Ga_{1-x}Mn_xAs$ films are under a very small (but finite) tensile strain from the ZnSe buffer, our data suggest that the easy axis of magnetization of all ferromagnetic $Ga_{0.99}Mn_{0.01}As$ films in Fig. 1 must be in the plane of the sample, so that our PMOKE measurements are actually determined by the hard axis of magnetization. One should note, however, that the data in Fig. 1 are not in contradiction with theoretical predictions: specifically, theoretical analysis indicates that the existence of an in-plane magnetic moment orientation can still occur for $Ga_{1-x}Mn_xAs$ layers under tensile strain as long as the strain is small.[20]

On the other hand, it is evident in the figure that the hysteresis profile of the samples evolves very systematically with increasing hole concentration. In particular, in the case of the sample with the lowest hole concentration (top left), the PMOKE curve resembles the magnetization curve for a uniaxial single-domain ferromagnetic film when the applied field is perpendicular to the easy axis of magnetization, except that the hysteresis is a tilted and elongated, with a small but finite remanent magnetization. We attribute the latter feature to domain wall movement during the process of magnetization reversal. As one follows the evolution of the M vs H curves with increasing hole concentration, the elongated hys-

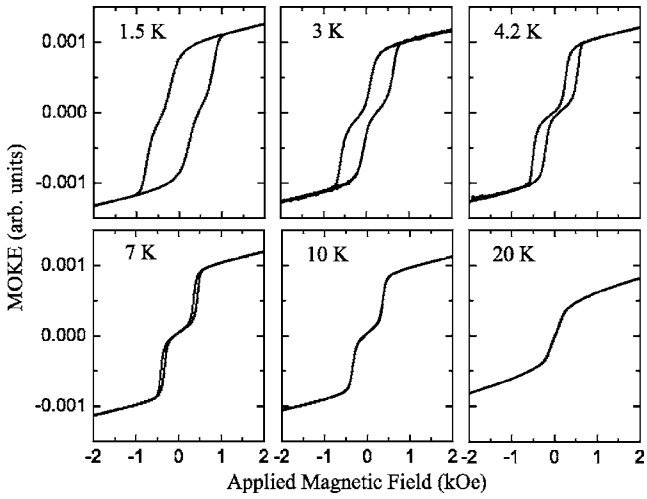

FIG. 2. Temperature evolution of the hysteresis curves revealed by PMOKE for a sample with $p=8.5\times10^{19}$ cm^{-3}.

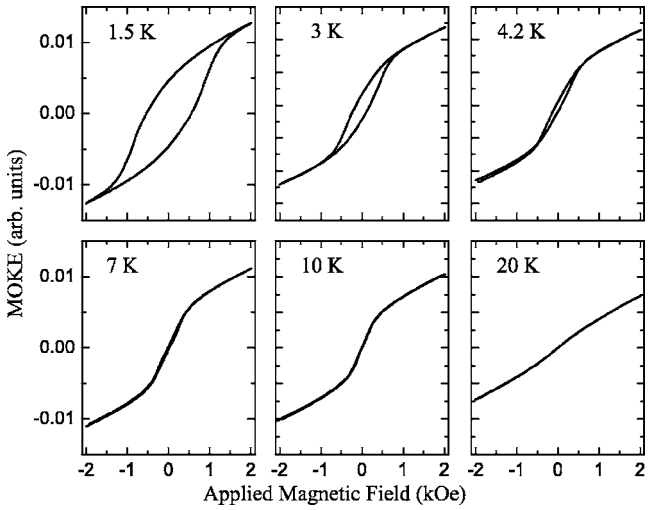

FIG. 3. Temperature evolution of the hysteresis curves revealed by PMOKE for a GaMnAs sample with $p=3.0\times10^{19}$ cm^{-3}.

teresis seen in the top left panel of Fig. 1 is gradually replaced with a double-hysteresis-loop feature occurring around 0.5 and −0.5 kOe, which becomes progressively more pronounced with increasing hole concentration p. Moreover, the remanent magnetization also disappears as p increases, indicating that the entire magnetic moment of the sample lies in the layer plane at zero field, as is typical for a ferromagnetic sample with uniform magnetization (i.e., for a single-domain system). We note parenthetically that such complex hysteresis profiles are usually observed in magnetic multilayer structures comprised of layers with different magnetic properties. In our case, however, as we will show later, the complicated hysteresis seen in Fig. 1 is recognized as an intrinsic property of the material. Specifically, it is an explicit manifestation of the fact that $Ga_{1-x}Mn_xAs$ layers are characterized by both uniaxial and cubic magnetocrystalline anisotropies which compete with each other, and the double hysteresis feature reflects the complicated form of the free energy density function that can have several local minima as a result of such competition.

Figure 2 follows the temperature evolution of the hysteresis loop for the sample with the highest hole concentration used in this study ($p=8.5\times10^{19}$ cm^{-3}). At higher temperatures (20 K) the low-field magnetization curve is evidently a straight line before it reaches saturation near $H\approx0.3$ kOe. As the temperature is lowered, the double-step feature already seen in Fig. 1 gradually evolves, with small hysteresis loops appearing and broadening around the two steps in the magnetization curve. With further decrease in temperature the broadening of these hysteresis loops gradually becomes the dominant feature, transforming the M vs H curve, so that at 1.5 K there is a significant remanent magnetization, with only a hint of the double-step feature superimposed on the nearly square hysteresis loop. The temperature progression of the hysteresis loop for the sample with the carrier concentration 4.4×10^{19} cm^{-3} looks quite similar, except that the double-step feature is much less pronounced. In the section that follows we will present arguments that the double-step hysteresis feature can be understood in terms of a complex magnetization reversal process combining coherent moment rotation, non-coherent moment switching, and domain nucleation and expansion.

Figure 3 shows the evolution of the hysteresis loop with temperature for the sample with the smallest hole concentration ($p=3.0\times10^{19}$ cm^{-3}), corresponding to the upper-left panel of Fig. 1. In this case no hint of the double-step feature can be found over the entire temperature range shown in the figure. Ignoring for the moment the hysteresis loop itself, one can see that near $H=0$ the magnetization *monotonically* increases with the applied magnetic field until it saturates—a typical behavior for a uniaxial specimen when the applied magnetic field is perpendicular to the easy axis of the magnetization. Note that when the temperature decreases, the remanent normal magnetization increases and the hysteresis loop becomes more pronounced. The latter effect may suggest a more complex incoherent mechanism of magnetization reversal, such as the presence of a large number of domains with different hystereses associated with chemical inhomogeneities or with dislocations in the crystal lattice.

In brief, from Figs. 1–3 one can see a rather dramatic difference of magnetic behavior evolving between $Ga_{1-x}Mn_xAs$ samples as a function of changing carrier concentration and temperature: the double-step magnetic reversal process is dominant when the carrier concentration is large; in contrast, this feature completely disappears when the carrier concentration is small. In addition, the width of the hysteresis loop (with or without the double-step feature) becomes systematically wider as the temperature decreases for all hole concentrations studied.

IV. DISCUSSION

A. Definition of relevant magnetic anisotropy terms

In order to understand the unusual shape of the hysteresis, and of its progression with carrier concentration and/or temperature in the present series of samples, we need to examine the various components of magnetic anisotropy that are expected to contribute to the magnetization of $Ga_{1-x}Mn_xAs$.

Although a comprehensive theory of magnetic anisotropy of $Ga_{1-x}Mn_xAs$ still needs to be developed, valuable insights into the properties of this system can be gained from a simple empirical model. A good starting point for this purpose is the Stoner-Wolfarth single homogeneous domain model.[21] In this model, for a given applied magnetic field H the direction of the magnetization is determined by the minima of the free energy density function, which takes into account the magnetocrystalline anisotropy. Within this framework, and with magnetic field applied perpendicular to the layer plane (i.e., along the [001] direction), the free energy density F for one of the easy planes of magnetization[22] [i.e., either the (010) or the (100) plane] can be expressed as follows:[7]

$$F = -MH\cos\theta + 2\pi M^2\cos^2\theta - \frac{M}{2}\left[H_{2\perp}\cos^2\theta + \frac{1}{2}H_{4\perp}\cos^4\theta + \frac{1}{2}H_{4\parallel}\sin^4\theta + \frac{1}{2}H_{2\parallel}\sin^2\theta\right]. \quad (1)$$

In this expression the first term is the Zeeman energy of the system in the applied magnetic field; θ is the angle between the sample normal (i.e., the [001] direction) and the magnetization vector; and the second term (the so-called "shape anisotropy") is usually quite small in the case of dilute ferromagnetic semiconductors due to their relatively low values of saturation magnetization (as compared to metallic ferromagnets).

The remaining four terms in Eq. (1) represent the combined effects of magneto-crystalline anisotropy, which is the subject of this study. Specifically, $H_{2\perp}$ is the perpendicular uniaxial anisotropy field resulting from the biaxial strain introduced during the MBE growth of $Ga_{1-x}Mn_xAs$ layers on substrates with a different lattice constant. $H_{2\parallel}$ is the in-plane uniaxial anisotropy stemming from the inequivalence of [110] and $[1\bar{1}0]$ directions, and is usually weak.[7,23] The terms $H_{4\perp}$ and $H_{4\parallel}$ represent the cubic anisotropy fields of zinc-blende $Ga_{1-x}Mn_xAs$. Cubic anisotropy, which reflects the inequivalence of the ⟨100⟩ and ⟨110⟩ directions, is dominant in the case of strain-free or very lightly strained $Ga_{1-x}Mn_xAs$. It is, however, extremely sensitive to the carrier concentration and temperature and—depending on the values of those parameters—it can favor either ⟨100⟩ or ⟨110⟩ as the easy axis of magnetization.[9,19] Since growth on a lattice-mismatched substrate introduces tetragonal distortion and breaks the purely cubic symmetry of the crystal lattice, the in-plane ($H_{4\parallel}$) and perpendicular ($H_{4\perp}$) cubic anisotropy fields need to be distinguished (they are of course equal in the limit of no strain).

In our samples the strain is expected to be quite small because of the small lattice mismatch between the ZnSe buffer and the $Ga_{0.99}Mn_{0.01}As$ layer, and therefore we expect the uniaxial anisotropy to be of the same order of magnitude as the cubic anisotropy. Additionally, in order to draw quantitative conclusions from the PMOKE data, it will be convenient to make two simplifying assumptions. First, since the in-plane uniaxial anisotropy $H_{2\parallel}$ is known to be significantly weaker than the uniaxial perpendicular and the cubic anisotropy fields for $Ga_{1-x}Mn_xAs$ films with low Mn concentration,[7] we will ignore the effects of this term. And second, because—as noted—the $Ga_{1-x}Mn_xAs$ layers in our series of samples are under very weak strain, we can also disregard the effect of the small tetragonal distortion of the crystal lattice on the cubic anisotropy parameters, and assume $H_{4\parallel}$ and $H_{4\perp}$ to be equal. In what follows we will then express both these terms simply as H_4. Finally, since the shape anisotropy and the perpendicular uniaxial anisotropy always appear together, we will treat them as a single term $(4\pi M - H_{2\perp})$.

B. Relation between magnetic anisotropy and magnetization reversal

In terms of the picture outlined above, it can be shown that the double-step form of the observed hysteresis curves is a consequence of the interplay between the anisotropy components $H_{2\perp}$ and H_4. The application of this model to the magnetization reversal in $Ga_{1-x}Mn_xAs$ layers is discussed in detail elsewhere.[24] Here we will only list the principal conclusions to which this model leads, and will use them to analyze the dependence of various anisotropy terms in our sample series on temperature and on carrier-concentration.

As shown in Fig. 4(a), at zero magnetic field the magnetization lies along the easy axis in the plane of the $Ga_{1-x}Mn_xAs$ layer (i.e., the free energy density has a minimum at $\theta = \pi/2$; see dashed curve in the figure). When the external magnetic field is applied normal to the layer, the minimum begins to shift, causing the magnetization to coherently rotate away from its in-plane orientation towards the normal. One can show from Eq. (1) that the normal component of the magnetization (i.e., the component which we measure by PMOKE) increases proportionally to the applied field with the slope[24]

$$\frac{dM_Z}{dH} = \frac{1}{(4\pi M - H_{2\perp} + H_4)}. \quad (2)$$

Also, in an applied field the local minimum at $\theta = 0°$ becomes increasingly pronounced as the field increases, as seen in Fig. 4(a). At a particular threshold magnetic field H_T the energies of the two local minima (at $\theta \sim 80°$ and $\theta = 0°$ become equal). This field can be expressed in terms of the anisotropy parameters as follows:[24]

$$H_T \approx (4\pi M - H_{2\perp} + H_4) - \sqrt{H_4(4\pi M - H_{2\perp} + H_4)}. \quad (3)$$

As long as the energy barrier that separates the two minima is sufficiently smaller than kT, it can be overcome by the process of domain nucleation and expansion with the aid of thermal excitations, and the magnetization will then align itself with the external magnetic field through incoherent moment switching.[24] At fields exceeding H_T the magnetization then remains oriented along the applied field, i.e., along $\theta = 0°$. When the field (which is normal to the sample plane) is decreased and then reversed, the magnetization first jumps back towards the in-plane orientation, and then again aligns itself with the applied field at $-H_T$. It is precisely those "jumps" at the characteristic fields H_T and $-H_T$ that explain the double-step profile observed in the hysteresis loop. To

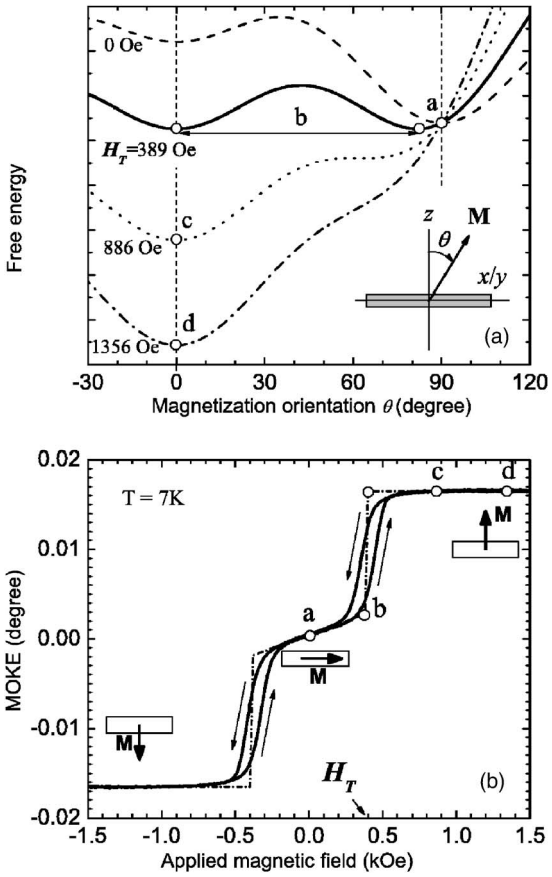

FIG. 4. Free energies plotted as the function of the angle θ between $\boldsymbol{M}$ and the sample normal for several fields (bottom panel). The initial status (i.e., "a") is set to $H=0$ Oe, $\theta=90°$; i.e., $\boldsymbol{M}$ is in the sample plane. As the applied field increases, the local energy minimum moves continuously to the applied field direction, $\theta=0°$, in the sequence of "a"-"b"-"c"-"d." The calculated perpendicular magnetization curve is plotted as a dash-dot curve in the bottom panel, with experimental data observed on the sample with the highest hole concentration shown as the solid curve. Note that at $H_T=389$ Oe the two local energy minima are equal.

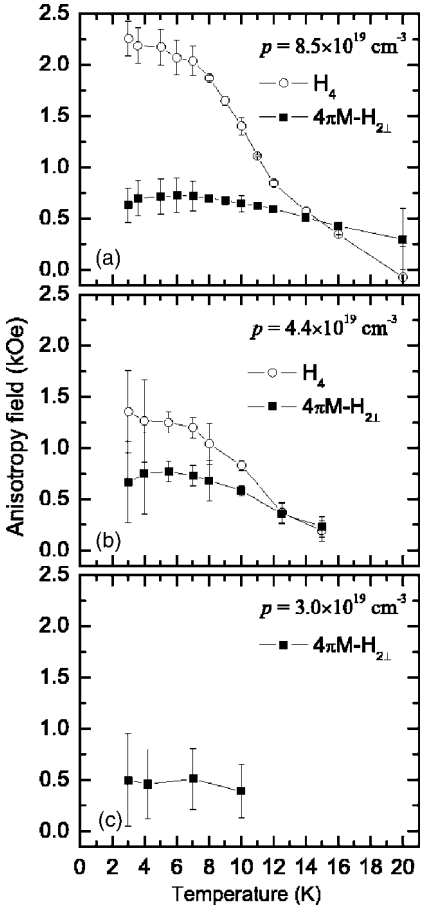

FIG. 5. Calculated values of the anisotropy fields as a function of temperature for the sample with (a) $p=8.5\times10^{19}$ cm^{-3}, (b) $p=4.4\times10^{19}$ cm^{-3}, and (c) $p=3.0\times10^{19}$ cm^{-3}.

illustrate this, we plot both the experimental data (solid curves) and the calculated magnetization (dash-dot curve) in Fig. 4(b).

We now address the occurrence of the hysteresis loops which accompany the step-like switching near $H=H_T$ and $-H_T$. In reality the jumps (i.e., the incoherent moment switching) do not occur simultaneously for all magnetic moments. Instead, reorientation of the magnetization is expected to take place by nucleating small regions (domains) with magnetization pointing in the direction that is determined by the lowest free energy minimum for that region, and by expansion of those regions. It is this complicated process that produces the hysteresis loops observed around the two switching fields H_T and $-H_T$. At lower temperatures, domain nucleation and the movement of domain walls becomes more difficult due to increased pinning and smaller thermal excitations, resulting in widening of the hysteresis loops and in increased overall coercivity, as seen in the experimental data (see, e.g., Fig. 2). We can determine both dM_Z/dH (i.e., the slope of the M vs H curve at $H=0$) and H_T (i.e., the center points of the hysteresis steps) from the PMOKE curves measured at different temperatures.

When the double-step feature is not present, so that the value of H_T is not defined, we can instead find the field at which the normal component of magnetization starts to decrease (relatively abruptly) from its saturation value as the external magnetic field is decreased.[24,25] We define this field as

$$H_N = 4\pi M - H_{2\perp} - H_4. \tag{4}$$

C. Dependence of magnetic anisotropy on hole concentration and temperature

Having determined the experimental parameters dM_Z/dH, H_T and H_N, we can now use Eqs. (2)–(4) to calculate the cubic (H_4) and perpendicular uniaxial ($4\pi M-H_{2\perp}$) anisotropy fields. The resulting fields are plotted as a function of temperature for the $Ga_{0.99}Mn_{0.01}As$ layer with hole concentrations 8.5×10^{19} cm^{-3}, 4.4×10^{19} cm^{-3}, and 3.0×10^{19} cm^{-3} in Fig. 5. The results for $p=3.4\times10^{19}$ cm^{-3} lie between those shown in the two lower panels of the figure, but much closer to the $p=3.0\times10^{19}$ cm^{-3} data, consistent with the trend which the figure illustrates. For the highest hole concentration, $p=8.5\times10^{19}$ cm^{-3}, the cubic anisotropy

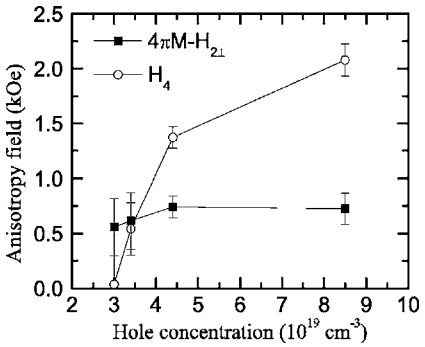

FIG. 6. Values of the anisotropy field for samples with different hole concentrations calculated from PMOKE data measured at 7 K.

term appears to be dominant at low temperatures. However, it drops rapidly as the temperature is increased. Perpendicular uniaxial anisotropy, on the other hand, is significantly less sensitive to the temperature, and surpasses the cubic anisotropy at temperatures close to T_C. As a result, at higher temperatures the double-step profile of the hysteresis disappears (see, e.g., 20 K curve in Fig. 2), and the magnetization curve shows the typical behavior observed in samples with only uniaxial anisotropy.

The temperature dependence of perpendicular uniaxial and cubic anisotropy components of the sample with $p=4.4\times10^{19}$ cm^{-3} in Fig. 5(b) looks qualitatively similar to that obtained for the sample with the highest hole concentration: the cubic anisotropy is stronger than uniaxial at low temperatures, but falls off more rapidly as the temperature increases. The magnitude of the uniaxial anisotropy in this sample is nearly the same as for $p=8.5\times10^{19}$ cm^{-3}, while the cubic anisotropy term is clearly smaller. For comparison, in Fig. 5(c) we also plot the temperature dependence of the perpendicular uniaxial anisotropy for the sample with lowest hole concentration, $p=3.0\times10^{19}$ cm^{-3}. Information on cubic anisotropy is difficult to obtain from the magnetization curves of this sample, and we estimate it to be near zero, since no double-step feature is observed for this sample, as seen in Fig. 3.

The temperature dependence of the resistivity observed on our $Ga_{0.99}Mn_{0.01}As$ sample series (p ranging from 3.0×10^{19} cm^{-3} to 8.5×10^{19} cm^{-3}; not shown here) shows a gradual transition with increasing p from clearly insulating behavior to somewhat metallic conductivity. Thus our measurements serve to illustrate how the magnetic anisotropy evolves at the point where the Fermi level in $Ga_{1-x}Mn_xAs$ just moves to the top of the valence band, and the holes are just becoming free from their acceptor centers.

Figure 6 shows the dependence of the cubic and uniaxial anisotropy fields on the hole concentration p, calculated using the PMOKE results for 7 K. While both anisotropy fields are relatively close in magnitude at low values of p, the cubic anisotropy field grows very rapidly with increasing p, and eventually outweighs the uniaxial anisotropy field. The strong dependence of H_4 on p is not surprising if we recall that the cubic anisotropy reflects the symmetry of the Fermi surface of the valence band, which is highly sensitive to the Fermi level.[19] The perpendicular uniaxial anisotropy field $4\pi M-H_{2\perp}$, on the other hand, shows only a very slight increase as the hole concentration increases by almost a factor of three. This is contrary to our expectation since according to earlier theoretical studies[18,19] the magnitude of the perpendicular uniaxial anisotropy is predicted to increases as the hole concentration increases. Although it is widely accepted that the perpendicular uniaxial anisotropy arises from symmetry changes of the hole Fermi surface induced by strain, our theoretical understanding of stress-induced effects on both the valence band (e.g., the effect of splitting of the heavy and light hole[18]) and on the impurity band (e.g., the splitting of the acceptor level[26,27]), is still far from complete for $Ga_{1-x}Mn_xAs$ with a low Mn concentration. Thus our data serve to illustrate the complexity of the hole band profile (including both valence and impurity band) for the $Ga_{1-x}Mn_xAs$ film with low Mn concentration.

For $Ga_{0.99}Mn_{0.01}As$ samples with low p, the holes are likely to be localized near the Mn^{++} ions and to form an impurity band, with the Fermi level positioned inside or near the impurity band. Under these conditions the hole-mediated ferromagnetic interaction is weak and short-range in character; and magnetocrystalline anisotropy is almost entirely dominated by the uniaxial term, originating most likely from stress-induced splitting of the acceptor lever. As the hole concentration increases, the Fermi level gradually moves into the top of valence band, the holes becoming increasingly free from their acceptor centers (i.e., increasingly delocalized). As the ferromagnetic interaction becomes stronger and acquires long-range character, the importance of the cubic magnetocrystalline anisotropy correspondingly increases. This increased prominence of the cubic anisotropy (i.e., the difference between the ⟨100⟩ and ⟨110⟩ directions) with hole concentration clearly reflects the four-fold symmetry of the Fermi surface at the top of valence band.

D. Origin of hysteresis loops at low temperature

Finally, it should be noted that—although the coercivity increases when the temperature decreases for all samples studied—the physical mechanisms which dominate their properties are in fact quite different from sample to sample. For the lowest hole concentration the holes are expected to become increasingly localized as the temperature approaches zero, and the material can then be classified as a short-range ferromagnet. Specifically, the material can then be regarded as composed of a large number of small ferromagnetic clusters (domains) with different magnetic properties (i.e., different anisotropies and hysteresis loops) due to disorder of the Mn ion distribution. In that case we observe a smooth (ovallike) hysteresis loop, in which the observed coercivity and remanence represent an average of the contributions from individual magnetic clusters (domains). As the temperature increases, the holes gradually become delocalized, thus increasing the long-range ferromagnetism (i.e., forming magnetic clusters of larger size) and the overall homogeneity of the specimen.

For samples with higher hole concentrations, on the other hand, i.e., when the holes are delocalized, the material becomes metallic, and can thus be categorized as a single-domain ferromagnet. As pointed out in Sec. IV A, however,

an exception to the idealized single-domain picture occurs during the magnetic switching near H_T and $-H_T$, i.e., when the applied magnetic field must move the domain wall through the material against various crystallographic obstacles (e.g., point and line defects). As the temperature approaches zero and thermal excitations diminish, the energy barrier between the two minima becomes more evident, and the magnitude of the field required to accomplish such switching becomes progressively larger [see Fig. 4(a)]. As a result, the hysteresis loops occurring at H_T and at $-H_T$ become gradually wider, and eventually merge into a single nearly-square hysteresis loop, with only residual kinks around the center, as seen in Fig. 1 at 1.5 K.

V. CONCLUSIONS

We studied magnetic anisotropy in thin $Ga_{1-x}Mn_xAs$ films in the regime of low Mn concentration, codoped by Be. The films were grown on ZnSe buffer layers, used to reduce the lattice-mismatch-induced strain in the magnetic film. In this condition the cubic and the uniaxial anisotropy fields in $Ga_{1-x}Mn_xAs$ become comparable, allowing us to study the interplay between the two for different values of hole concentration p and temperature T. Our experimental results demonstrate that the cubic anisotropy field H_4 decreases rapidly with temperature, and is very sensitive to the value of the hole concentration. In sharp contrast, the perpendicular uniaxial anisotropy field $H_{2\perp}$ remains relatively unaffected by T and/or p. The different T and/or p dependences for uniaxial and cubic anisotropy fields of thin $Ga_{0.99}Mn_{0.01}As$ films illustrates the complexity of the Fermi surface of the holes in this material, reflecting the combined effects of the valence and the impurity bands. This work has shown that, by appropriately choosing the strain and the hole concentration, we can achieve a regime where the cubic and the uniaxial anisotropy mechanisms can be made to compete, providing a handle for manipulating the process of magnetization reversal by appropriately adjusting the sample temperature.

ACKNOWLEDGMENT

This work was supported by NSF Grants DMR 02-10519 and DMR 02-45227.

*Electronic address: mdobrowo@nd.edu

[1] H. Ohno, Science **281**, 951 (1998).
[2] H. Ohno, J. Magn. Magn. Mater. **200**, 110 (1999).
[3] D. Chiba, M. Yamanouchi, F. Matsukura, and H. Ohno, Science **301**, 943 (2003).
[4] S. T. B. Goennenwein, T. A. Wassner, H. Huebl, M. S. Brandt, J. B. Philipp, M. Opel, R. Gross, A. Koeder, W. Schoch, and A. Waag, Phys. Rev. Lett. **92**, 227202 (2004).
[5] X. Liu, W. L. Lim, M. Dobrowolska, J. K. Furdyna, and T. Wojtowicz, Phys. Rev. B **71**, 035307 (2005).
[6] M. Sawicki, F. Matsukura, A. Idziaszek, T. Dietl, G. M. Schott, C. Ruester, C. Gould, G. Karczewski, G. Schmidt, and L. W. Molenkamp, Phys. Rev. B **70**, 245325 (2004).
[7] X. Liu, Y. Sasaki, and J. K. Furdyna, Phys. Rev. B **67**, 205204 (2003).
[8] G. P. Moore, J. Ferré, A. Mougin, M. Moreno, and L. Däweritz, J. Appl. Phys. **94**, 4530 (2003).
[9] M. Sawicki, F. Matsukura, T. Dietl, G. M. Schott, C. Ruester, G. Schmidt, L. W. Molenkamp, and G. Karczewski, J. Supercond. **16**, 7 (2003).
[10] D. Hrabovsky, E. Vanelle, A. R. Fert, D. S. Yee, J. P. Redoules, J. Sadowski, J. Kanski, and L. Ilver, Appl. Phys. Lett. **81**, 2806 (2002).
[11] U. Welp, V. K. Vlasko-Vlasov, X. Liu, J. K. Furdyna, and T. Wojtowicz, Phys. Rev. Lett. **90**, 167206 (2003).
[12] We obtain this estimate from x-ray diffraction measurements, which give an in-plane lattice parameter of 6.663 Å for the partially relaxed ZnSe buffer. The lattice parameter of (relaxed) $Ga_{0.99}Mn_{0.01}As$ is estimated to be 5.656 Å.
[13] Note that, although in principle such addition of Be to the GaMnAs lattice should lead to a slight reduction of the lattice parameter, which could have an additional effect on strain, our x-ray diffraction measurements indicate the effects on the lattice constant to be imperceptible at the Be doping levels used in the present investigation.
[14] D. Ruzmetov, J. Scherschligt, D. V. Baxter, T. Wojtowicz, X. Liu, Y. Sasaki, J. K. Furdyna, K. M. Yu, and W. Walukiewicz, Phys. Rev. B **69**, 155207 (2004).
[15] K. Shinagawa, in *Magneto-Optics*, edited by S. Sugano and N. Kojima (Springer-Verlag, Heidelberg, 2000).
[16] R. Lang, A. Winter, H. Pascher, H. Krenn, X. Liu, and J. K. Furdyna, Phys. Rev. B **72**, 024430 (2005).
[17] A. Shen, A. Oiwa, A. Endo, S. Katsumoto, Y. Iye, H. Ohno, F. Matsukura, Y. Sugawara, N. Akiba, and T. Kuroiwa, J. Cryst. Growth **175/176**, 1069 (1997).
[18] M. Abolfath, T. Jungwirth, J. Brum, and A. H. MacDonald, Phys. Rev. B **63**, 054418 (2001).
[19] T. Dietl, H. Ohno, and F. Matsukura, Phys. Rev. B **63**, 195205 (2001).
[20] See Fig. 11 in T. Dietl, H. Ohno, and F. Matsukura, Phys. Rev. B **63**, 195205 (2001).
[21] E. C. Stoner and E. P. Wohlfarth, Philos. Trans. R. Soc. London, Ser. A **240**, 74 (1948).
[22] Since $H_{4\|}>0$ and $|H_{4\|}| \gg |H_{2\|}|$ for the $Ga_{1-x}Mn_xAs$ specimens under study (i.e., the [100] and [010] direction are the easy axes of magnetization), for any given θ_H the equilibrium condition will be $\varphi=\varphi_H=0°$ or 90°, i.e., the magnetization will be constrained to move only in (010) and (100) planes. We will refer to these planes as "easy planes of magnetization."
[23] K. Hamaya, T. Taniyama, Y. Kitamoto, R. Moriya, and H. Munekata, J. Appl. Phys. **94**, 7657 (2003).
[24] X. Liu, W. L. Lim, L. V. Titova, M. Dobrowolska, J. K. Furdyna, M. Kutrowski, and T. Wojtowicz, cond-mat/0505322.
[25] R. A. Hyman, A. Zangwill, and M. D. Stiles, Phys. Rev. B **58**, 9276 (1998).
[26] M. Linnarsson, E. Janzén, B. Monemar, M. Kleverman, and A. Thilderkvist, Phys. Rev. B **55**, 6938 (1997).
[27] V. F. Sapega, M. Moreno, M. Ramsteiner, L. Däweritz, and K. Ploog, Phys. Rev. Lett. **94**, 137401 (2005).